

ARTICLE OPEN



VEGF-A, PDGF-BB and HB-EGF engineered for promiscuous super affinity to the extracellular matrix improve wound healing in a model of type 1 diabetes

Michael J. V. White¹, Priscilla S. Briquez¹, David A. V. White² and Jeffrey A. Hubbell^{1,3,4}✉

Chronic non-healing wounds, frequently caused by diabetes, lead to lower quality of life, infection, and amputation. These wounds have limited treatment options. We have previously engineered growth factors to bind to exposed extracellular matrix (ECM) in the wound environment using the heparin-binding domain of placental growth factor-2 (PIGF-2_{123–144}), which binds promiscuously to ECM proteins. Here, in the type 1 diabetic (T1D) NOD mouse model, engineered growth factors (eGFs) improved both re-epithelialization and granulation tissue formation. eGFs were even more potent in combination, and the “triple therapy” of vascular endothelial growth factor-A (VEGF-PIGF-2_{123–144}), platelet-derived growth factor-BB (PDGF-BB-PIGF-2_{123–144}), and heparin-binding epidermal growth factor (HB-EGF-PIGF-2_{123–144}) both improved wound healing and remained at the site of administration for significantly longer than wild-type growth factors. In addition, we also found that changes in the cellular milieu of a wound, including changing amounts of M1 macrophages, M2 macrophages and effector T cells, are most predictive of wound-healing success in the NOD mouse model. These results suggest that the triple therapy of VEGF-PIGF-2_{123–144}, PDGF-BB-PIGF-2_{123–144}, and HB-EGF-PIGF-2_{123–144} may be an effective therapy for chronic non-healing wounds in that occur as a complication of diabetes.

npj Regenerative Medicine (2021)6:76; <https://doi.org/10.1038/s41536-021-00189-1>

INTRODUCTION

Diabetes is a major health scourge that affects more than 415 million people worldwide. One in eleven adults has diabetes, and 12% of all global health expenditures are related to diabetes¹, including chronic non-healing diabetic wounds. The risk for diabetic patients to develop lower extremity non-healing wounds ranges from 15% to 25% during their lifetime^{2,3}, and about 33% of the direct costs of diabetes are linked with the treatment of diabetic foot ulcers⁴.

Type 1 diabetes (T1D) affects 1.25 million Americans, 5% of diabetics overall, and primarily manifests in children⁵. T1D is the most prevalent form of diabetes in youth and accounts for more than 85% of young diabetic patients⁵. Further, T1D has been increasing in global incidence by 3% annually⁵. Although T1D has only 5–10% of the prevalence of type 2 diabetes (T2D), the health complications for T1D are more severe^{6,7}, with persons with T1D heal both acute and chronic wounds poorly, independent of their glycemic control⁸.

Chronic non-healing wounds affect more than 6.5 million US patients per year, which is approximately 2% of the population, and cost more than \$25 billion to treat⁹. Compared to healthy wounds, chronic non-healing wounds exhibit poor resolution of the inflammatory phase of wound healing¹⁰. This includes impaired leukocyte recruitment and phagocytic activity and increased concentrations of pro-inflammatory cytokines^{11,12}.

The extracellular matrix (ECM) is a highly dynamic structure that modulates cell proliferation, migration, and differentiation during the course of wound healing¹³. During wound healing, immune cells and fibroblasts secrete various growth factors (GFs) in the wound, most of which interact with ECM before finding their cognate cell surface receptors. The ECM sequesters GFs, which

creates a slow-release reservoir of GF for local signaling^{14,15}. ECM composition and secreted GFs create a signaling microenvironment that tightly controls cellular responses in the healing wound¹³. This signaling environment changes as the wound heals, as do the types of cells interacting in the wound¹⁶.

Due to an excessively proteolytic environment, chronic non-healing wounds have a fragmented ECM structure, which results in poor sequestration of GFs. In addition, the high protease activity in chronic wounds digests GFs and GF receptors at an increased rate¹⁷. Together, the dysregulated ECM and increased proteolysis of chronic non-healing wounds disorganize cellular behavior (i.e., migration, proliferation, differentiation) and prevent wound resolution, since proper cellular orchestration is key to resolving each stage of wound healing¹³.

GFs are potent biological signals that can instruct cell morphology, metabolism, and differentiation. GFs have been hindered as medical treatments due to off-target signaling^{13,18}, low signaling efficacy, and high expenses due to the high concentration of GFs necessary to overcome the off-target signaling and low signaling efficacy^{19,20}.

Platelet-derived growth factor-BB (PDGF-BB) is one of the first GFs to be released into the wound environment by platelet degranulation and is subsequently secreted by monocyte-derived cells, fibroblasts, and endothelial cells in later stages of wound healing^{21–23}. PDGF-BB thus plays an important role in multiple subsequent stages of wound healing. Particularly, PDGF-BB promotes the development of granulation tissue within the wound via its effects on fibroblast proliferation, mesenchymal stem cell (MSC) recruitment and ECM production²¹.

Vascular endothelial growth factor-A (VEGF-A) is responsible for angiogenesis in wounds by triggering the angiogenic cascade^{24,25}.

¹Pritzker School of Molecular Engineering, University of Chicago, Chicago, IL 60615, USA. ²Department of Mathematics and Computer Science, Denison University, Granville, OH 43023, USA. ³Committee on Immunology, University of Chicago, Chicago, IL 60615, USA. ⁴Committee on Cancer Biology, University of Chicago, Chicago, IL 60615, USA. ✉email: jhubbell@uchicago.edu

On a cellular level, VEGF interacts with monocyte-derived cells and endothelial cells through the VEGF-receptor-2 (VEGFR2) to create new blood vessels within granulation tissue^{24,26}. Like PDGF-BB, VEGF-A is released through subsequent wound stages by multiple cell types, including platelets, monocyte-derived cells, fibroblasts, and endothelial cells²⁶.

Heparin-binding epidermal growth factor (HB-EGF) has increased secretion in damaged skin²⁷ and is secreted by macrophages²⁸. HB-EGF operates through epidermal growth factor receptor (EGFR, also called human epidermal growth factor receptor 1, HER1)²⁷, affects keratinocyte proliferation and migration (dependent on dose and means of presentation^{29–31}), and accelerates wound re-epithelization²².

While several GFs play roles in wound healing^{21,32}, PDGF-BB, VEGF-A, and HB-EGF are especially promising as drug targets due to their signaling potency and ability to interact with multiple cell types in the wound environment^{22,33}.

Recombinant GFs have been explored in human trials as topical treatments for diabetic foot ulcers: PDGF-BB³⁴, VEGF-A (NCT00351767), and HB-EGF (NCT01629199). Of these, only PDGF-BB has thus far been approved for human use as the topical gel Regranex. However, Regranex, which is used at a rather high dose of 7 µg/cm² and is applied daily for up to 2 weeks³⁵, carried a warning about potential carcinogenic effects due to the potential for recombinant PDGF-BB to escape into the bloodstream and cause distant tumors through off-target signaling³⁶.

Thus, the development of a delivery approach that reduces off-target signaling of GFs and increases the local concentration of GF at appropriate sites of tissue regeneration could be highly beneficial for GF-based tissue regeneration therapies. Previously, we engineered growth factors (eGFs) that promiscuously bind to ECM proteins in wounds¹⁹, by fusing them to the heparin-binding domain from placental growth factor-2 (-PIGF-2_{123–144}). These eGFs speed wound healing, can be used at lower concentrations, and thus may be safer than wild-type (WT) GFs¹⁹. Indeed, we showed that the eGFs have increased retention at the site of application as a result of binding to the ECM¹⁹. Increased retention at the site of application reduces the risk of eGFs escaping into the blood or lymphatic system and causing off-target effects.

Wound healing is a complex process in which a multitude of cell types migrate, differentiate, and proliferate in an environment of complex secreted signals and ECM surfaces. Further, this cellular milieu changes as the wound heals, with each successive change bringing the wound closer to resolution through the inflammatory, proliferative, and remodeling phases of wound healing^{37,38}. Thus, understanding the cellular milieu of wounds is essential for a mechanistic understanding of eGF's effect on wounds.

The initial inflammatory stage of wound healing are characterized by neutrophil infiltration, and neutrophil persistence in wounds is key to the inflammation within the wound. This stage of wound healing lasts for a period of hours up to days after wounding¹⁶.

The proliferation phase of wound healing begins after the inflammatory stage begins, and is characterized by infiltration of MSCs, smooth muscle cells, endothelial cells, and macrophages¹⁹. The tissue remodeling phase usually begins 1–3 days after wounding³⁹, and includes the T cell response to the wound¹⁶. Macrophages are key effectors of wound healing⁴⁰, secreting several cytokines and GFs, and mediating the differentiation and proliferation of several types of cells in the wound.

Macrophages in a wound differentiate into several different types: classically activated macrophages (M1 macrophages) are key to perpetuating inflammation and phagocytosing cell debris in the wound⁴¹. Alternatively activated (M2) macrophages are responsible for tissue remodeling⁴¹. Arginase is an enzyme that catalyzes the production of ornithine and urea, and arginase-positive macrophages promote wound healing⁴². The presence and appropriate differentiation of macrophages within a wound is

essential for the restoration of tissues, and arginase-positive macrophages are necessary for proper wound healing⁴². Under-scoring macrophage importance in healing wounds, depletion of macrophages from a wound inhibits wound healing⁴³.

Non-hematopoietic cells are also key to wound regeneration. Particularly, endothelial cells are key to lining new blood vessels, and MSCs form the basis of much of wound healing through their ability to differentiate into multiple cell types¹⁶.

If wounds remain unhealed for enough time, the adaptive immune system can begin to affect the outcome of the wound¹⁶. Amphiregulin is an autocrine GF, and amphiregulin-positive tissue-repair T cells are a newly discovered class of T cells that are important for wound healing^{42,44}. T-regulatory cells (Tregs) are anti-inflammatory cells, and removal of Tregs slows wound closure⁴⁵.

The diabetic-specific problems of non-healing chronic wounds (abnormal glycation in the wound environment, increased proteolytic activity, and poor ECM sequestration) considerably reduce the signaling efficacy of locally produced GFs on the cell behavior in a wound (proliferation, migration, and differentiation). This cellular dysregulation disrupts the resolution of the inflammatory, proliferative, and remodeling phases of wound healing^{37,38}. Because eGFs bind strongly to the exposed ECM, they are sequestered in the ECM of chronic non-healing wounds and protected from proteolysis better than are recombinant WT GFs. This dysregulated environment makes eGFs a promising treatment for delivering GFs potent signaling to the wound environment.

RESULTS

Co-delivery of VEGF-A-PIGF-2_{123–144}, PDGF-BB-PIGF-2_{123–144}, and HB-EGF-PIGF-2_{123–144} improves wound healing

We previously observed that the PIGF-2_{123–144} domain was a promiscuous binder of multiple ECM proteins¹⁹. Co-delivery of engineered VEGF-A-PIGF-2_{123–144} and PDGF-BB-PIGF-2_{123–144} improved re-epithelialization more than co-delivery of VEGF-A and PDGF-BB in the T2D db/db mouse model. Here, we sought to extend this work to a T1D model using the NOD mouse, and to explore addition of a third eGF, namely HB-EGF-PIGF-2_{123–144}.

To model T1D wound healing in manner relevant to a clinical setting, we allowed NOD mice to become diabetic spontaneously, then treated them until their glucose was suboptimally controlled with insulin, then wounded them. To determine if GF or eGF (GF-PIGF-2_{123–144}) can improve wound healing in the T1D NOD model, we added 200 ng of VEGF-A, PDGF-BB, and HB-EGF (GF and eGF variants) to wounded skin.

While no GF or eGF increased granulation tissue until 7 days (Fig. 1a, c), co-administration of VEGF and PDGF-BB improved the re-epithelialization of NOD wounds at both 3 and 7 days (Fig. 1b, c). The addition of HB-EGF resulted in an increase in granulation tissue as compared to wounds treated with fibrin alone after 1 week (Fig. 1c). Treatment with the triple therapy (VEGF-A-PIGF-2_{123–144}, PDGF-BB-PIGF-2_{123–144}, and HB-EGF-PIGF-2_{123–144}) increased both wound closure and granulation tissue compared to the NOD control mouse, and also compared to the non-diabetic NOD variant NOR mouse (Fig. 1c, d). Further, the triple therapy eGFs outperformed the WT variants (Fig. 1c, d) in both granulation tissue formation and wound closure. eGF triple therapy did not outperform GF therapy based on specific activity, because both GF and eGF both activate their receptors to equivalent extents (Fig. 2a). eGFs are, however, retained in wounded tissue at higher concentrations for significantly longer time than the corresponding GF (Fig. 2b). By way of comparison with our previous study¹⁹ with VEGF-A-PIGF-2_{123–144}, PDGF-BB-PIGF-2_{123–144} combination in the db/db T2D model, the eGF triple therapy led to more granulation tissue (Fig. 1c) and more

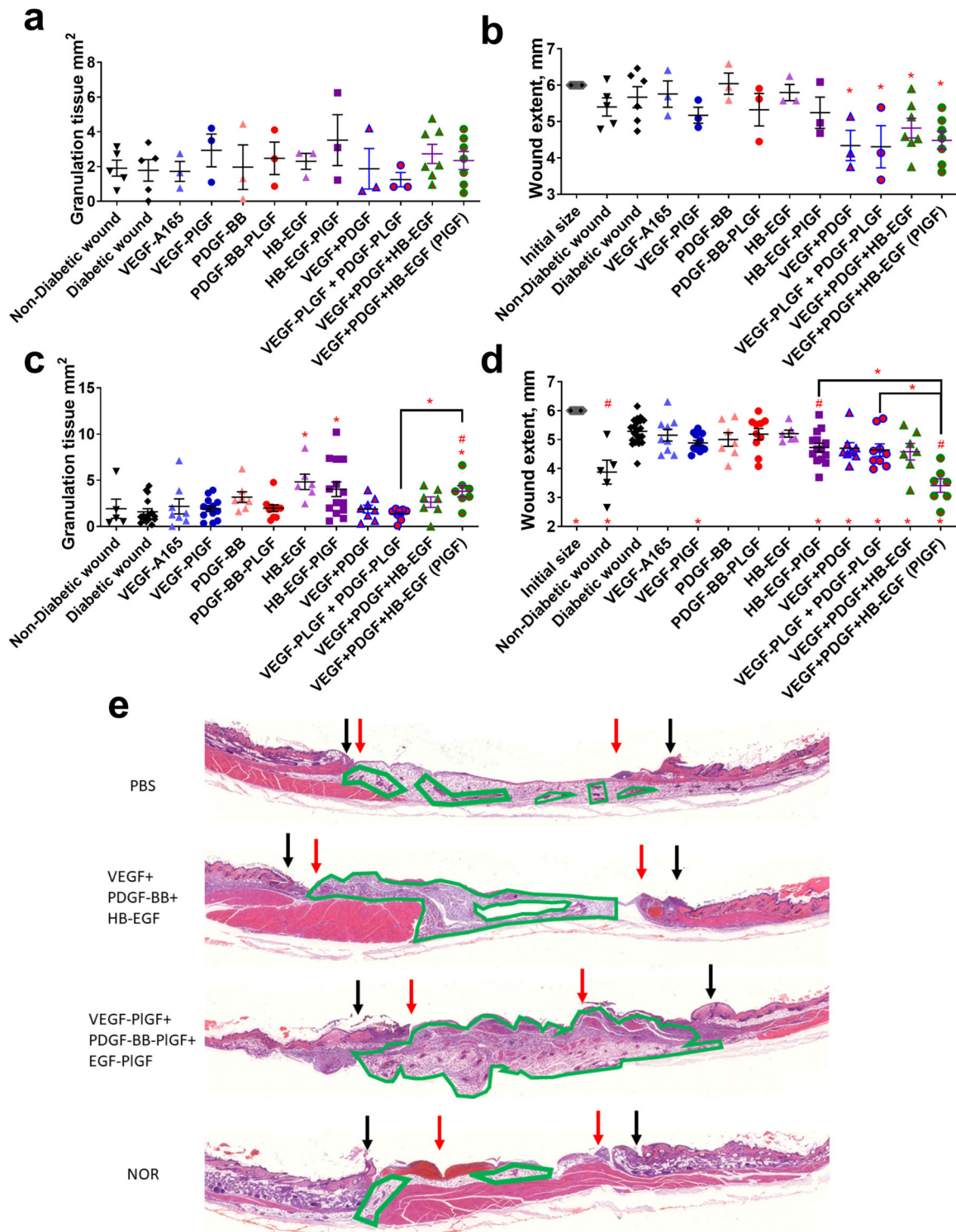


Fig. 1 The triple therapy of VEGF-PIGF-2₁₂₃₋₁₄₄, PDGF-BB-PIGF-2₁₂₃₋₁₄₄, and HB-EGF-PIGF-2₁₂₃₋₁₄₄ improves wound healing in the T1D NOD mouse model. Given as measured by increased granulation-tissue formation (a, c) and wound extent (diameter of unhealed wound normalized to the known length of the resection biopsy punch (12 mm) to account for folding or contraction of wound tissue (b, d)). Time points assayed are 3 days (a, b) and 7 days (c, d). For wound extent, smaller numbers indicate more healing. e Representative images of healed wounds from 7 days, stained with hematoxylin and eosin. Black arrows indicate initial wound extent, red arrows indicate healed extent. Scale bar is 1 mm. *n* ranges from 3 to 20. * Denotes comparison to the diabetic wound. # Denotes a comparison between untreated NOD wound and untreated NOR wound, and the WT GF(s) are compared to their counterpart -PLGF-2₁₂₃₋₁₄₄ variant(s), e.g., VEGF vs VEGF-PIGF-2₁₂₃₋₁₄₄. **p* < 0.05, *p* < 0.01, *p* < 0.001, ANOVA + Student's *t*-test for post hoc for wound extent, Kruskal-Wallis + Mann-Whitney post hoc test for granulation tissue. #*p* < 0.05, *p* < 0.01, *p* < 0.001, Mann-Whitney for granulation tissue, Student's *t*-test for wound extent. Student's *t*-test for comparison between VEGF-PIGF₁₂₃₋₁₄₄ + PDGF-PIGF₁₂₃₋₁₄₄ and VEGF-PIGF₁₂₃₋₁₄₄ + PDGF-PIGF₁₂₃₋₁₄₄ + HB-EGF-PIGF₁₂₃₋₁₄₄. Error bars are SEM.

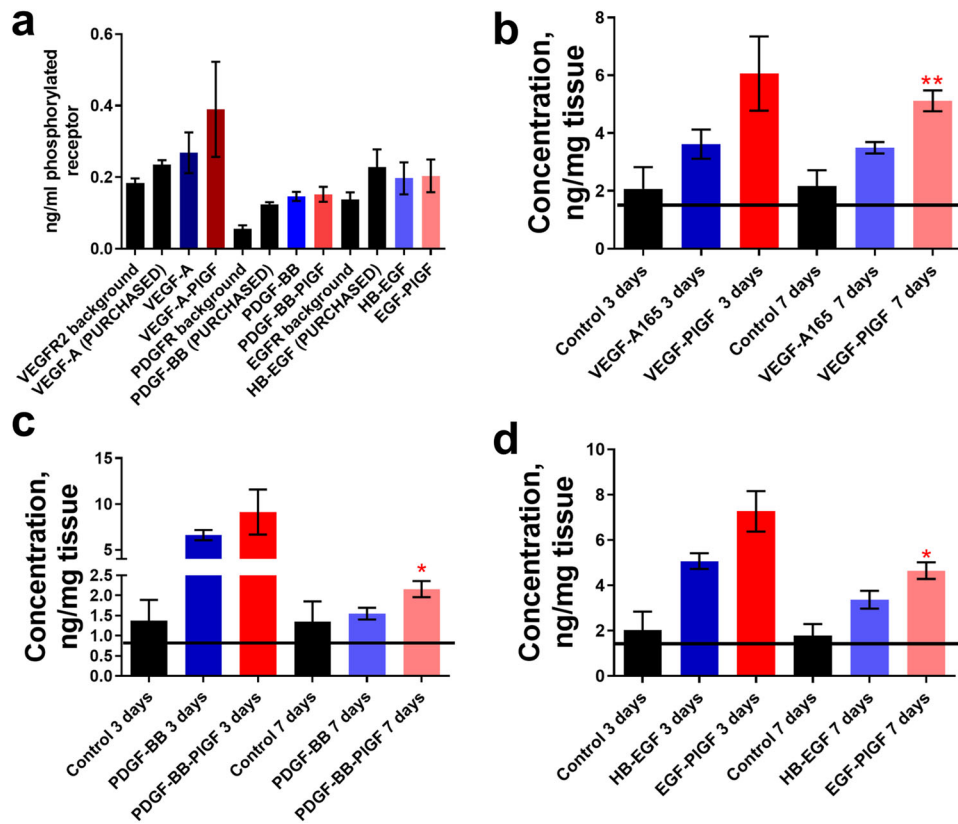


Fig. 2 Growth factors fused with the -PLGF-2₁₂₃₋₁₄₄ activate their cognate receptors at levels comparable to WT GF and remain in wound tissue longer than their wild-type (WT) counterpart. **a** 100 ng of VEGF-A-PIGF-2₁₂₃₋₁₄₄, PDGF-BB-PIGF-2₁₂₃₋₁₄₄, and HB-EGF-PIGF-2₁₂₃₋₁₄₄ caused corresponding receptor phosphorylation (VEGFR2, PDGFR, and EGFR, respectively) at the indicated amounts over 10 min on HUVEC cells (for VEGF-A165) or fibroblasts (for PDGF-BB and HB-EGF). Concentrations in wounded skin tissue (ng/mg) for **(b)** VEGF-A-PIGF-2₁₂₃₋₁₄₄, **(c)** PDGF-BB-PIGF-2₁₂₃₋₁₄₄, and **(d)** HB-EGF-PIGF-2₁₂₃₋₁₄₄ after the indicated time points. $n = 7$, $p < 0.05$, Mann-Whitney. Error bars are SEM.

extensive wound closure (Fig. 1d) at 7 days than did the dual combination therapy. The eGF triple therapy was also more efficacious than HB-EGF-PIGF-2₁₂₃₋₁₄₄ by this measure (Fig. 1d). Figure 1e and Fig. S1 show representative histology staining of wound sections.

Diabetic covariates are not predictive of wound outcomes in the mouse walk-in clinic

Interestingly, mouse-specific diabetic covariates (age, previous glucose high, glucose reading at the time of surgery, see Table 1), are not predictive of wound-healing outcomes (wound extent or granulation tissue), as indicated by a higher R^2 value or by a lower p -value. Rather treatment with the triple therapy of eGFs (VEGF-A-PIGF-2₁₂₃₋₁₄₄, PDGF-BB-PIGF-2₁₂₃₋₁₄₄, and HB-EGF-PIGF-2₁₂₃₋₁₄₄) is more predictive of wound-healing outcomes (Table 1). This suggests that the combination of these eGFs may be more useful treatments than GF in a clinical setting. The cellular milieu of wounds changes through the stages of wound healing¹⁶. Non-healing diabetic wounds can become stuck in a non-resolving inflammatory cycle¹⁶. To determine if eGF treatment works through changing the cellular composition of the wounds, we analyzed cellular compositions of the wounds by flow cytometry at days 3 and 7 post wounding. The triple therapy treatment significantly decreased the number of neutrophils at both time points, to levels comparable to non-diabetic NOR mouse wounds (Fig. 3a, b). The eGFs of the triple therapy also outperformed the WT variant of triple therapy in neutrophil reduction (Fig. 3a). Neutrophils are pro-inflammatory cells, and the reduction of neutrophils has been reported to be key to breaking the inflammatory cycle in non-healing wounds¹⁶.

Triple therapy eGF treatment changes the cellular milieu of the healing wound

Following neutrophils (which can arrive at the wound in a matter of hours) are macrophages, which arrive and differentiate at the wound site over multiple days. Macrophages consist of many subtypes, some of which are inflammatory and others that are anti-inflammatory¹⁶. Treatment with the triple therapy increases the ratio of these anti-inflammatory macrophages to pro-inflammatory macrophages (Fig. 4a, b). The -PIGF-2₁₂₃₋₁₄₄ variant (VEGF-PIGF-2₁₂₃₋₁₄₄, PDGF-BB-PIGF-2₁₂₃₋₁₄₄, and HB-EGF-PIGF-2₁₂₃₋₁₄₄) of the triple therapy increased the ratio compared to -WT variants (VEGF, PDGF-BB, and HB-EGF) of the triple therapy (Fig. 4a, b).

Arginase is an enzymatic component of the urea cycle that is upregulated in wound-healing macrophages. Treatment with the -PIGF-2 variant triple therapy (VEGF-PIGF-2₁₂₃₋₁₄₄, PDGF-BB-PIGF-2₁₂₃₋₁₄₄, and HB-EGF-PIGF-2₁₂₃₋₁₄₄) increases the number of arginase-positive wound-healing macrophages at 7 days post wound healing (Fig. 4d), as compared to diabetic wounds. The triple therapy (VEGF-PIGF-2₁₂₃₋₁₄₄, PDGF-BB-PIGF-2₁₂₃₋₁₄₄, and HB-EGF-PIGF-2₁₂₃₋₁₄₄) does not increase the number of arginase-positive inflammatory M1 macrophages, and in fact significantly decreases the overall number of inflammatory M1 macrophages in wounds (Fig. 4a, b).

Non-hematopoietic stromal cells are also key in wound healing. The triple therapy (VEGF-PIGF-2₁₂₃₋₁₄₄, PDGF-BB-PIGF-2₁₂₃₋₁₄₄, and HB-EGF-PIGF-2₁₂₃₋₁₄₄) did not increase the number of MSC after 3 days (Fig. 5a), but increased the number of MSC at 7 days (Fig. 5b) and increased the number of endothelial cells at both 3 and 7 days (Fig. 5c, d). The -PIGF-2₁₂₃₋₁₄₄ variant of triple therapy

Table 1. Statistical comparison of cell number in wound, correlated with wound-healing outcome.

Variable	R^2 for wound closure	R^2 for granulation tissue
Mouse age	$R^2 = -0.001314, p = 0.358$	$R^2 = 0.0009965, p = 0.2935$
Glucose average	$R^2 = 0.006687, p = 0.1881$	$R^2 = -0.008086, p = 0.7504$
>400 mg/dl glucose previously	$R^2 = -0.002706, p = 0.4018$	$R^2 = -0.009239, p = 0.9155$
Treatment (with GF or eGF)	$R^2 = 0.2279, p = 0.0001654$	$R^2 = 0.1762, p = 0.001831$
Neutrophils	$R^2 = -0.01028, p = 0.8547$	$R^2 = -0.01062, p = 0.9696$
Endothelial cells	$R^2 = 0.016, p = 0.0922$	$R^2 = 0.01237, p = 0.122$
Mesenchymal stem cells	$R^2 = 0, p = 0.3031$	$R^2 = -0.0006868, p = 0.3391$
M1 macrophages	$R^2 = 0, p = 0.3252$	$R^2 = 0.02836, p = 0.05507$
M2 macrophages	$R^2 = 0.01307, p = 0.136$	$R^2 = 0.08148, p = 0.0028$
M2 macrophages arginase positive	$R^2 = -0.01, p = 0.909$	$R^2 = 0.058, p = 0.01$
T regulatory cells	$R^2 = 0, p = 0.97$	$R^2 = 0.05267, p = 0.0139$
M1/M2 ratio	$R^2 = -0.01, p = 0.904$	$R^2 = 0.0017, p = 0.284$
Treatment + M2.Arg macrophages + neutrophils + all interaction terms	$R^2 = 0.1719, p = 0.01013$ (w/o interaction); $R^2 = 0.1508, p = 0.2054$ (with)	$R^2 = 0.56, p = 0.0002$ (w/ all interaction terms)
Effector T cells	$R^2 = 0.036, p = 0.03$	$R^2 = -0.01074, p = 0.9714$
Effector T cells and M1 macrophages	$R^2 = 0.02885, p = 0.0967$	$R^2 = 0.01813, p = 0.1603$
Treatment × Neutrophils × Mesenchymal.Stem.Cells × Effector (notation means all interaction terms)	$R^2 = 0.9799, p = 0.0037$	
Treatment × M2.Arg.vs.all.mac × Neutrophils × Mesenchymal.Stem.Cells		$R^2 = 0.8821, p = 0.04862$

Linear models using data on the cellular makeup of wounds (Figs. 3–8) and mouse-specific covariates (age, average glucose at time of wounding, and previous high glucose reading >400 mg/dl) as explanatory variables and wound outcomes (wound extent or granulation tissue) as the response, using scatterplots to confirm the linear relationship. R^2 measures the percentage of variance in the response variable explained by the explanatory variables. Adjusted R^2 includes a penalty term for models with too many variables. * $P < 0.05$, ** $P < 0.01$, *** $P < 0.001$.

significantly increases the number of MSC and endothelial cells at 7 days compared to the WT variants (Fig. 5b, d).

MSC localization can also be used to measure the amount of vascularization in the wound environment, since MSC surround newly developed vascular tissue⁴⁶. Immunofluorescence for MSC indicates an increase of MSC staining in triple-therapy-treated wounds, though this increase is not significant (Fig. S2). Treatment with triple therapy (VEGF-PIGF-2_{123–144}, PDGF-BB-PIGF-2_{123–144}, and HB-EGF-PIGF-2_{123–144}) also increased the number of proliferating cells in the wound significantly (Fig. S3) when compared to both untreated diabetic wounds and to diabetic wounds treated with untargeted triple therapy.

The adaptive immune system participates in the later stages of wound healing¹⁶. Several GFs (including the triple therapy) decrease the number of CD4⁺ T cells that are amphiregulin positive (Fig. 6d). The triple therapy (VEGF, PDGF-BB, and HB-EGF) in both -WT and -PIGF-2_{123–144} variants decrease the number of effector T cells at 1 week after treatment, with no significant difference between one another (Fig. 7c). Treatment by GF or eGF do not significantly change the number of Tregs in the wound after 3 and 7 days (Fig. 8a, b), though they do decrease the amounts of amphiregulin-positive cells after 3 and 7 days (Fig. 8c, d).

The numbers of M1 macrophages, M2 macrophages, and effector T cells correlate with wound outcome

Since we treated the mice in a simulation of a walk-in clinic (where each mouse is treated as it individually becomes diabetic, and where each mouse is given insulin therapy adapted to its glycemic state), we can statistically compare the mouse-specific variables (age, previous glucose high-level, glucose level during wound healing) and cell concentrations (neutrophils, macrophages, MSCs,

epithelial cells, and effector T cells) with wound-healing outcomes (granulation tissue and re-epithelialization) (Table 1). For a traditional linear regression model, the R^2 value measures the percentage of variance in the response variable explained by the explanatory variable.

Interestingly, the variable with the highest R^2 value for predicting wound-healing outcome was the eGF treatment added. For wound extent the triple therapy treatment produced an adjusted R^2 of 0.2279.

Individual cell types that significantly predicted wound-healing outcomes were M2 macrophages and effector T cells, which both significantly correlated with increased granulation tissue (Table 1). Of the mouse-specific variables measured (mouse age, glucose average before wounding and before sacrifice, and whether the mouse achieved a glucose level of more than 450 mg/dl previously), none significantly predicted wound-healing outcomes (wound closure or granulation tissue).

While the number of specific types of cells can correlate with wound-healing outcomes in some cases, in other cases a combination of cell number and location is key to the wound-healing outcomes. Multivariate linear regression models including both the treatment and the percentages of cells improved the predictive power for wound outcomes. For granulation tissue, the best model (with an R^2 of 0.556, a substantial improvement over treatment alone which has an R^2 of 0.17) used treatment, percentage of M2 macrophages, and percentage of neutrophils. Including interaction terms did not improve the R^2 of the model. For wound extent, the best model (with an R^2 of 0.32, a substantial improvement over treatment alone which has an R^2 of 0.23) used treatment, percentage of effector T cells, and percentage of M1 macrophages. For wound extent, there is a significant interaction. Leaving out the interaction terms resulted in an R^2 of only 0.26.

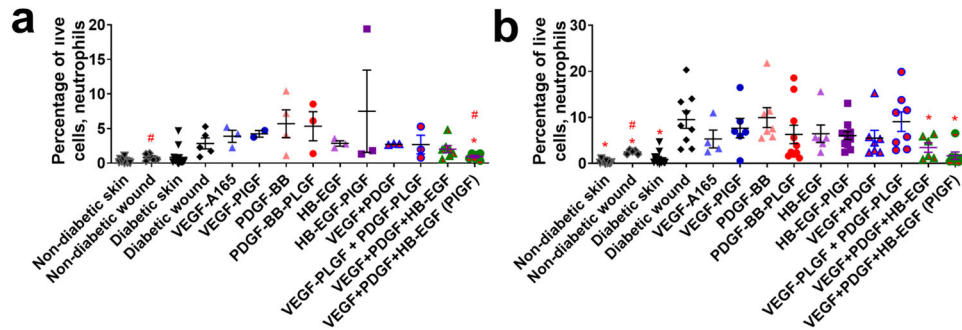


Fig. 3 Neutrophil (CD45⁺, CD11b⁺, CD11c⁻, Ly6G⁺) count in wounds after 3–7 days of healing. a 3 days, b 7 days. Comparison includes unwounded skin from both the NOD and NOR mice. *n* ranges from 3 to 20. * Denotes comparison to the diabetic wound. # Denotes a comparison between untreated NOD wound and untreated NOR wound, and the WT GF(s) are compared to their counterpart placental growth factor (-PLGF-2₁₂₃₋₁₄₄) variant(s), e.g., VEGF vs VEGF- PiGF-2₁₂₃₋₁₄₄. **p* < 0.05, *p* < 0.01, *p* < 0.001, Kruskal-Wallis + Mann-Whitney post hoc test. #*p* < 0.05, *p* < 0.01, *p* < 0.001, Mann-Whitney. Error bars are SEM.

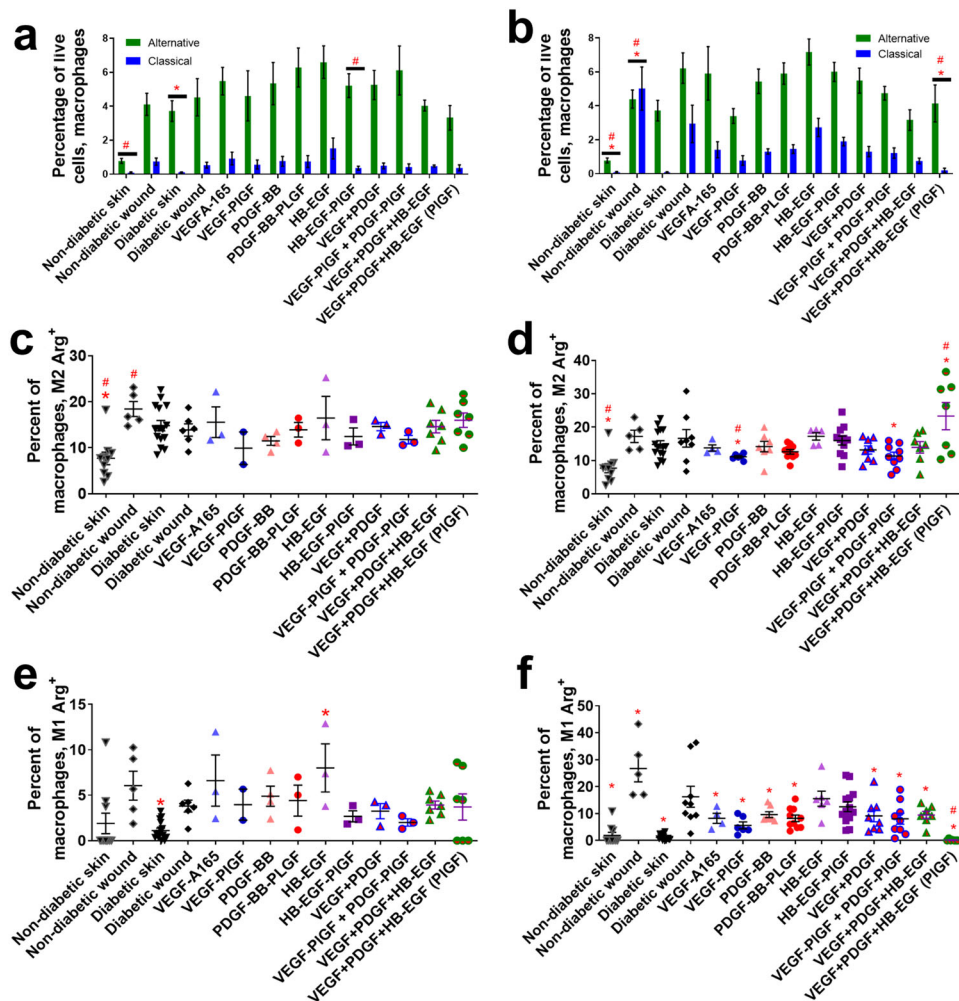


Fig. 4 Macrophage cell count in wounds after 3–7 days of healing. Inflammatory M1 (CD45⁺, CD11b⁺, CD11c⁻, Ly6G⁻, Ly6C^{low}, SSC^{high}, MHC class II⁺) vs alternatively activated M2 (CD45⁺, CD11b⁺, CD11c⁻, Ly6G⁻, Ly6C^{high}, SSC^{low}, CD206⁺) macrophages after (a) 3 days or (b) 7 days. Arginase⁺ alternatively activated macrophages after (c) 3 days or (d) 7 days. Arginase⁺ classically activated macrophages after (e) 3 days or (f) 7 days. Comparison includes unwounded skin from both the NOD and NOR mice. *n* ranges from 3 to 20. * Denotes comparison to the diabetic wound. # Denotes a comparison between untreated NOD wound and untreated NOR wound, and the WT GF(s) are compared to their counterpart -PLGF-2₁₂₃₋₁₄₄ variant(s), e.g., VEGF vs VEGF- PiGF-2₁₂₃₋₁₄₄. **p* < 0.05, *p* < 0.01, *p* < 0.001, Kruskal-Wallis + Mann-Whitney post hoc test. #*p* < 0.05, *p* < 0.01, *p* < 0.001, Mann-Whitney. Error bars are SEM.

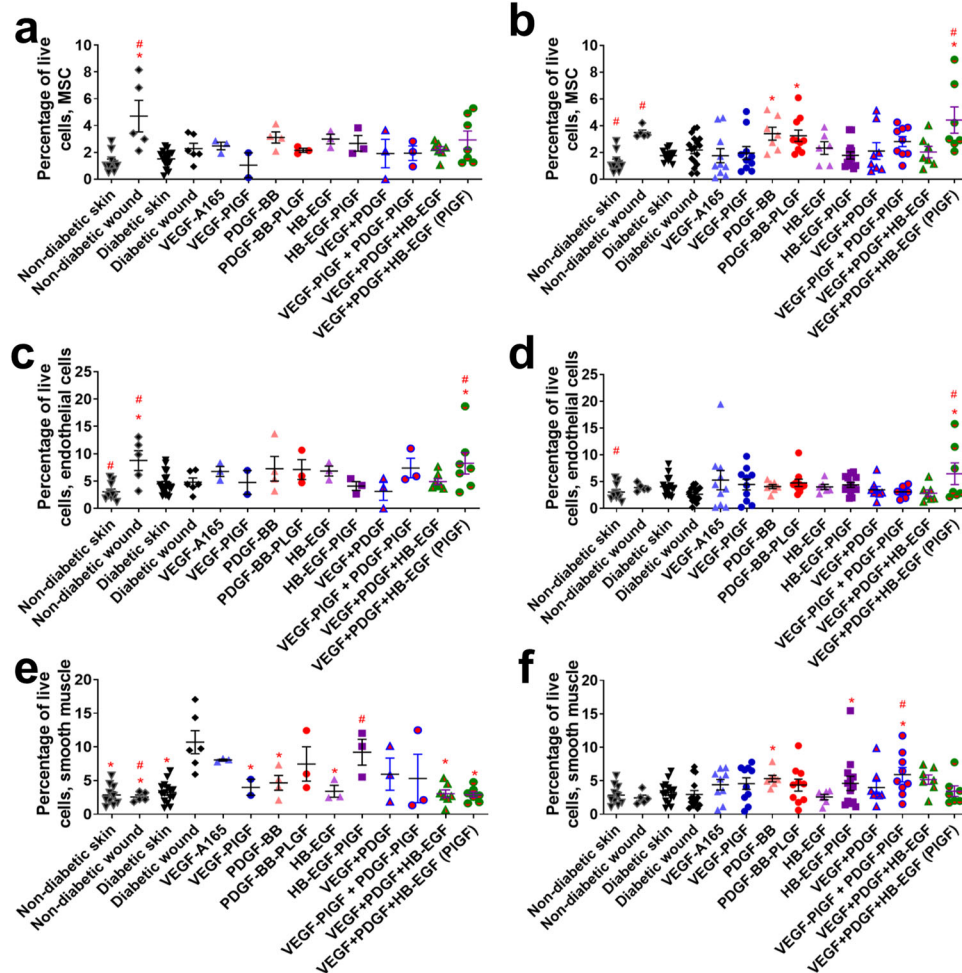


Fig. 5 Non-hematopoietic cell count in wounds after 3–7 days of healing. Mesenchymal stem cells (CD45⁻, CD44⁺, CD29⁺, CD90⁺, SCA-1⁺) after (a) 3 days or (b) 7 days. Endothelial cells (CD45⁻, CD31⁺) after (c) 3 days or (d) 7 days. Smooth muscle cells CD45⁻, SMA⁺) after (e) 3 days or (f) 7 days. Comparison includes unwounded skin from both the NOD and NOR mice. *n* ranges from 3 to 20. # Denotes a comparison between untreated NOD wound and untreated NOR wound, and the WT GF(s) are compared to their counterpart -PLGF-2_{123–144} variant(s), e.g., VEGF vs VEGF-PIGF-2_{123–144}. **p* < 0.05, *p* < 0.01, *p* < 0.001, Kruskal-Wallis + Mann-Whitney post hoc test. #*p* < 0.05, *p* < 0.01, *p* < 0.001, Mann-Whitney. Error bars are SEM.

DISCUSSION

We previously demonstrated that co-administration of VEGF-A and PDGF-BB (and especially their -PIGF-2_{123–144} eGF variants) improves re-epithelialization in the mouse T2D db/db mouse model¹⁹. The present study considers three questions: first, whether the eGF triple therapy treatment (VEGF-A-PIGF-2_{123–144}, PDGF-BB-PIGF-2_{123–144}, and HB-EGF-PIGF-2_{123–144}) has a statistically significant effect on wound healing for mice with T1D; second, whether addition of HB-EGF-PIGF-2_{123–144} to the dual combination was beneficial; and third, the specific way in which the cellular milieu of a wound affects healing upon treatment.

Here we demonstrate that eGF triple therapy significantly improves measurements both re-epithelialization and granulation tissue in the NOD mouse model of T1D, and that addition of HB-EGF-PIGF-2_{123–144} to the regimen is indeed beneficial (Fig. 1). The eGF triple therapy also operates at doses far lower than previously approved GF therapeutics. Regranex's dose of PDGF-BB for the treatment of diabetic foot ulcers is 7 µg/cm² (or 1800 ng/28 mm²), administered daily for 2 weeks³⁵, is far greater than our dose of 200 ng/28 mm², administered once. Additionally, presentation of GFs in an sequestered, ECM-bound state can change their signaling properties. Immobilized HB-EGF preferentially causes

keratinocyte migration, while soluble HB-EGF preferentially causes keratinocyte proliferation³⁰.

The NOD model develops T1D via a similar immunological sequence as in human disease⁴⁷. Our NOD colony was allowed to develop T1D without induction, permitting us to operate a model “walk-in wound clinic”, which resulted in data on the age, weight, and glucose history of each mouse in our study. These mouse-specific covariates had less influence on the outcome of the wounds (re-epithelialization and granulation tissue) than the GF or eGF treatments (Table 1), or the cellular milieu of the wounds (Table 1), based on their *R*² values. While mice age affects its hair growth⁴⁸, we did not find a statistical relationship between mouse age and response to wounding (Table 1), suggesting the most important variables in wound healing were the GF treatment added to the wound, not the severity of the glucose dysregulation, the duration of the diabetes, or the age of the mice.

While healing wounds undergo changes in their cellular milieu¹⁶, the cellular composition of a wound changes based on treatment with GFs and eGFs (Figs. 3–8). This cellular milieu can be correlated with wound-healing outcomes.

The cell populations with the highest *R*² values for wound outcomes (re-epithelialization and granulation tissue) are M1 macrophages, M2 macrophages, and effector T cells (Table 1).

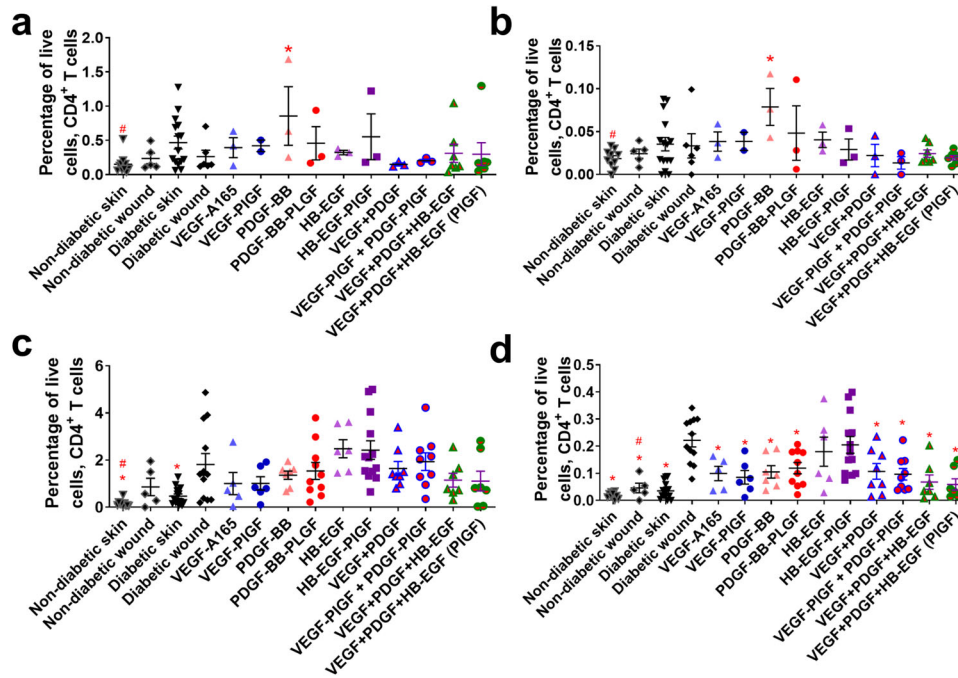


Fig. 6 CD4⁺ T cell count in wounds after 3–7 days of healing. CD4⁺ T cells (CD45⁺, CD3⁺, CD4⁺) at (a) 3 days or (c) 7 days. Subset of CD4⁺ T cells that are amphiregulin positive at (b) 3 days or (d) 7 days. Comparison includes unwounded skin from both the NOD and NOR mice. *n* ranges from 3 to 20. * Denotes comparison to the diabetic wound. # Denotes a comparison between untreated NOD wound and untreated NOR wound, and the WT GF(s) are compared to their counterpart -PLGF-2_{123–144} variant(s), e.g., VEGF vs VEGF-PLGF-2_{123–144}. **p* < 0.05, *p* < 0.01, *p* < 0.001, Kruskal-Wallis + Mann-Whitney post hoc test. #*p* < 0.05, *p* < 0.01, *p* < 0.001, Mann-Whitney. Error bars are SEM.

Interestingly, while GF and eGF triple therapy treatment of wounds significantly affected the number of neutrophils and MSCs, neither of these cell types are predictive of improved wound outcomes on their own (Table 1). These findings contradict previous wound studies that have found MSCs to be integral to wound healing⁴⁹. This discrepancy could be explained by the fact that several studies have found that MSCs are less functional in diabetic wounds, and that in these cases, additions of MSC-conditioned media may contribute to better wound outcomes⁴⁹.

eGF treatment significantly changed the ratio between M1 and M2 macrophages, but this change is not predictive of improved wound outcome (Table 1). These results could indicate that changes in the number of certain cells in a wound might be an outcome of improved wound healing, as opposed to a cause of improved wound healing.

Intriguingly, the opposite can also be true. The numbers of Tregs were not significantly increased by GF or eGF treatment, but Tregs did have a small but significant correlation with increased granulation tissue formation (Table 1). This indicates that triple therapy treatment improves wound healing using only some of the total constellation of available cell types and interactions within wounds. Depletion of Tregs slows wound closure in a non-diabetic model⁴⁵. In the NOD diabetic mouse strain, dendritic cells are defective in their presentation to T cells, which could potentially explain why Tregs were not predictive of wound closure in our model⁵⁰. Interestingly, dendritic cell function is restored in NOR mice⁵¹.

Also interestingly, all seven wounds treated with the triple therapy eGFs had zero M1 macrophages or zero effector T cells, suggesting that the lowered number of inflammatory cells might be key to improved wound outcomes. However, when correlated (Table 1), lower numbers of effector T cells correlate with improved re-epithelialization, and do not appear to affect granulation tissue formation. Lower numbers of M1 macrophages, conversely, correlate with increased granulation tissue formation, and do not appear to affect re-epithelialization.

Combining cellular data and treatment data (as variables) improved predictive outcomes for wound healing (Table 1). Since many factors go into successful wound healing, it is unreasonable to expect that any combination of explanatory variables would produce an R^2 value of 1, i.e., completely explain the response variable. For multivariate regression models, additional explanatory variables can only ever increase the R^2 value. To avoid models with too many explanatory variables, the adjusted R^2 value includes a penalty term that increases with the number of variables. Hence, adding a useless variable will result in a smaller adjusted R^2 . Further, cross-validation ensured these models were not overfit to the data.

The fact that the eGFs with the -PLGF-2_{123–144} domain improve wound healing in comparison to the WT GFs at 7 days, but less so at 3 days, is mirrored in several of the datasets. The eGFs remain in the wound at higher concentrations at 1 week in comparison to the WT GF, and there is no significant difference at 3 days. There are also more significant differences in an eGF-treated wound's cellular milieu after 7 days of healing in comparison to the GF-treated wounds, or NOD or NOR control wounds. The few differences in the wound's cellular milieu at day 3 support the hypothesis that the longer duration of the eGFs in wounds improves wound healing, and that the individual eGFs are not intrinsically more potent signaling proteins than GF. These findings suggest that different cell types are responsible for different kinds of healing, either inducing re-epithelialization or increasing the granulation tissue in a wound.

METHODS

Fusion growth factor design

WT human GFs (VEGF-A165, PDGF-BB, and HB-EGF) were selected for their varied effects on the wound environment, and their potential synergy for combination. Sequences obtained from Genscript (Piscataway, NJ, USA) were transferred into pXLG¹⁹, and the sequence for PLGF-2's heparin-binding domain (-PLGF-2_{123–144}) was substituted for the native heparin-

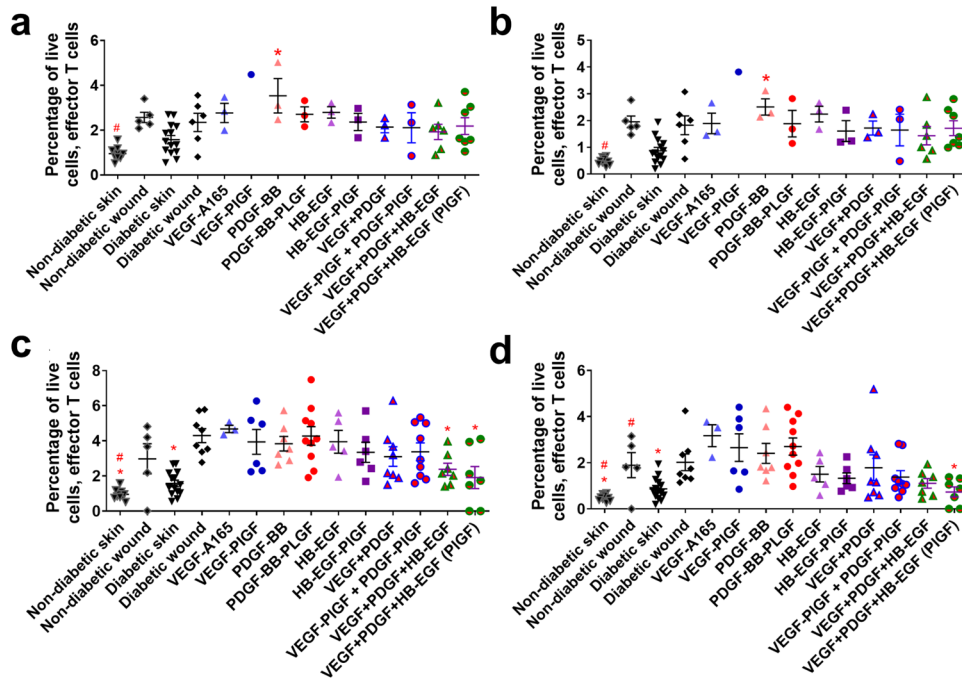


Fig. 7 Effector T cell count in wounds after 3–7 days of healing. Effector T cells (CD45+, CD3+, CD44+, CD62L–) at (a) 3 days or (c) 7 days. Subset of effector T cells that are amphiregulin positive at (b) 3 days or (d) 7 days. Comparison includes unwounded skin from both the NOD and NOR mice. *n* ranges from 3 to 20. * Denotes comparison to the diabetic wound. # Denotes a comparison between untreated NOD wound and untreated NOR wound, and the WT GF(s) are compared to their counterpart -PLGF-2_{123–144} variant(s), e.g., VEGF vs VEGF-PIGF-2_{123–144}. **p* < 0.05, *p* < 0.01, *p* < 0.001, ANOVA + Student *t*-test for post hoc. #*p* < 0.05, *p* < 0.01, *p* < 0.001, Student's *t*-test. Error bars are SEM.

binding domains of VEGF-A165 and HB-EGF, and was added to the C-terminus of PDGF-BB, resulting in the GFs denominated as VEGF-A-PIGF-2_{123–144}, PDGF-BB-PIGF-2_{123–144}, and HB-EGF-PIGF-2_{123–144}. All GFs were his-tagged at the N-terminus.

Growth factor production

WT and fusion GF were produced by transfection of human embryonic kidney HEK-293f cells, and purified by his tag affinity to a nickel column (HisTrap, GE healthcare, Chicago, IL, USA) via fast protein liquid chromatography (FPLC), as previously described¹⁹. GFs were assessed for purity by gel electrophoresis (>95%), and tested negative for endotoxins by a HEK-mouse TLR4 blue assay, as previously described¹⁹. GF concentration was assessed by bicinchoninic acid assay (BCA), according to the manufacturer's directions (Thermo, Waltham, Massachusetts).

Growth factor-receptor phosphorylation assay

Human endothelial cells from umbilical vein (ATCC, Manassas, VA, USA) and MRC5 fibroblasts (ATCC) were serum starved overnight and stimulated with GFs, as previously described¹⁹. Cells were then lysed, and that lysate was assayed for GF receptor phosphorylation via DuoSet ELISA kits (R&D Systems, Minneapolis, MN, USA) for VEGFR2, PDGFR, and EGFR, as per the manufacturer's instructions.

Mouse walk-in clinic

The mice used in this study were non-obese diabetic (NOD) and control mice of the same background that do not develop diabetes (NOR). The mouse colony was maintained in-house, and blood glucose levels of the females were assessed weekly starting at 8 weeks old. Mice were defined as diabetic when they had two readings over 250 mg/dl or one reading over 400 mg/dl. To maintain glycemic control, albeit suboptimally, diabetic mice were treated with 1–2 insulin pellets (Linshin, Scarborough, Ontario, Canada) per the manufacturer's instructions. Specifically, the back of diabetic mice were shaved and sterilized with iodine and alcohol wipes. Following that, Linshin insulin pellets were placed in sharpened 12 gauge needles and pellets were placed subcutaneously in the mouse back. One pellet was used for mice with glucose readings between 300 mg/dl and 500 mg/dl, and two pellets were used for mice with glucose readings

greater than 500 mg/dl. In order to proceed to the wounding phase of the study, the mice had to have stabilized glucose levels between 250 mg/dl and 300 mg/dl for 2 subsequent weeks.

Mouse wounding and healing

All animal experiments were performed with protocols approved by the University of Chicago IACUC. Wounding was performed as previously described⁵². Specifically, mice were anesthetized by 2% isoflurane. Mouse backs were shaved and sterilized with alcohol and iodine wipes. Two symmetrical wounds were made per mouse using a 6 mm biopsy punch. Sterile siliconized rubber splints were sewn onto the skin surrounding the wound using a suture kit. Wounds were then treated with GFs suspended in fibrin gel, bandaged with clear bandages, and wrapped with band aids to prevent scratching. Mice were monitored daily, and no signs of infection were observed during this study.

Wounds were resected after euthanasia (3 or 7 days of healing) with a 12 mm biopsy punch to keep the resection conditions consistent. Wounds were fixed in 4% paraformaldehyde, mounted in paraffin, and sectioned into 5 μm sections at the widest point of the wound. Wounds were then stained with hematoxylin and eosin. Wound extent and granulation tissue were assessed as previously described¹⁹.

Retention of GF in wounded tissue

Half of the full thickness wound was mechanically disrupted with a tissue homogenizer in the presence of protease inhibitors, as previously described¹⁹. Briefly, a 12 mm biopsy punch of a wound was cut in half with a razor blade. Half of the wound was frozen, and then wounds from the study were thawed, and mechanically ground in a tissue homogenizer (MP Biomedicals, Santa Ana, California) utilizing lysing matrix D (MP Biomedicals) in the presence of an EDTA-free protease inhibitor cocktail (Thermo). The amount of VEGF, PDGF-BB, and HB-EGF (WT and -PLGF-2_{123–144} variants) present in the tissue lysate were assessed by ELISA (DuoSet, R&D Systems), per the manufacturer's instructions.

Flow cytometry

Half of a wound was mechanically disrupted by maceration, digested with 1 μg/ml collagenase-d (Sigma) for 1 h with shaking, and frozen in 10%

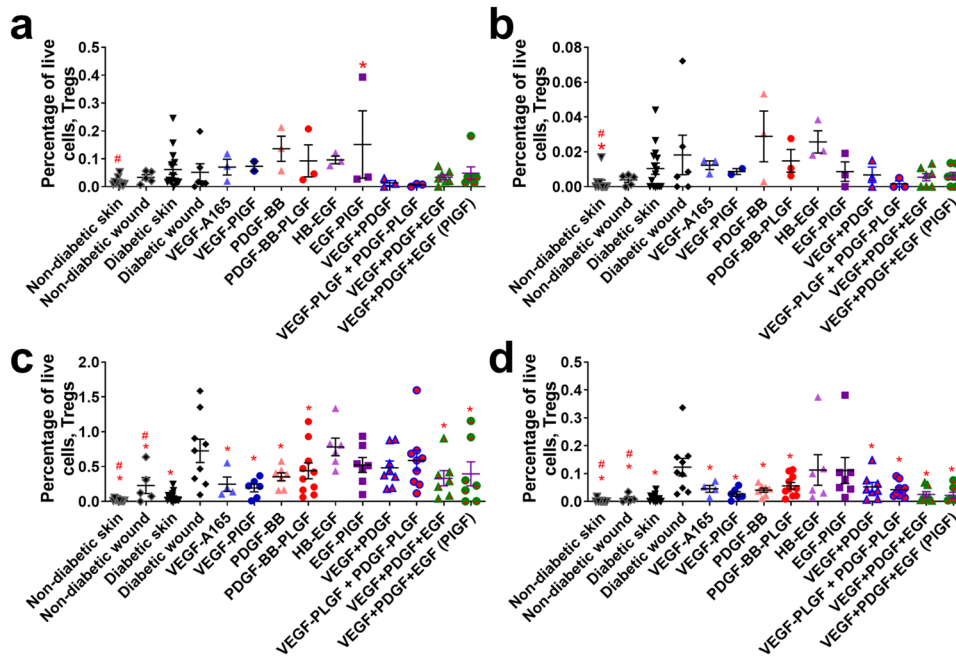


Fig. 8 T regulatory cell count in wounds after 3–7 days of healing. T-regulatory cells (CD45⁺, CD3⁺, CD4⁺, CD25 high, Foxp3⁺) at (a) 3 days or (c) 7 days. Subset of effector T cells that are amphiregulin positive at (b) 3 days or (d) 7 days. Comparison includes unwounded skin from both the NOD and NOR mice. *n* ranges from 3 to 20. * Denotes comparison to the diabetic wound. # Denotes a comparison between untreated NOD wound and untreated NOR wound, and the WT GF(s) are compared to their counterpart -PLGF-2_{123–144} variant(s), e.g., VEGF vs VEGF-PIGF-2_{123–144}. **p* < 0.05, *p* < 0.01, *p* < 0.001, Kruskal-Wallis + Mann-Whitney post hoc test. #*p* < 0.05, *p* < 0.01, *p* < 0.001, Mann-Whitney. Error bars are SEM.

dimethylsulfoxide (DMSO). All samples were thawed and analyzed via flow cytometry at the same time, to create greater consistency within the flow cytometry data. Digested wound tissue was split into three equal portions and stained for flow cytometry based on panels for the following: non-hematopoietic cells, innate immune cells, and adaptive immune cells.

Live-dead stain was live-dead aqua, used per manufacturer's instructions (ThermoFisher). Compensation was performed via UltraComp beads (ThermoFisher) per the manufacturer's instructions. The panels used to identify cells were: neutrophils (CD45⁺, CD11b[−], CD11c[−], Ly6G⁺), M1 inflammatory macrophages (CD45⁺, CD11b⁺, CD11c[−], Ly6G[−], Ly6C⁺, MHC class II⁺), M2 wound-healing macrophages (CD45⁺, CD11b⁺, CD11c[−], Ly6G[−], Ly6C⁺, CD206⁺), MSCs (CD45[−], CD44⁺, CD29⁺, CD90⁺, SCA-1⁺), endothelial cells (CD45⁺, CD31⁺), CD4 T cells (CD45⁺, CD3⁺, CD4⁺), CD8 T cells (CD45⁺, CD3⁺, CD8⁺), naive T cells (CD45⁺, CD3⁺, CD44[−], CD62L⁺), central memory T cells (CD45⁺, CD3⁺, CD44⁺, CD62L⁺), effector T cells (CD45⁺, CD3⁺, CD44⁺, CD62L[−]), regulatory T cells (Treg; CD45⁺, CD3⁺, CD4⁺, CD25 high, Foxp3⁺), Th2: CD45⁺, CD3⁺, CD4, gata-3. Antibodies against arginase, amphiregulin and ki-67 were also added, where appropriate.

Immunofluorescence

Paraffin-fixed 7-day wounds were sectioned to 5 mm. Antigen retrieval was performed using citrate buffer. Primary antibodies (CD73 (647), CD90 (488)⁴⁶), were added at 5 mg/ml overnight. Wounds were washed 3x in PBS, and were exposed to DAPI (ThermoFisher) for 1 min. Cells were mounted using diamond anti-fade mounting media (ThermoFisher) to preserve fluorescence. Slides were imaged immediately using a confocal microscope (Olympus, Shinjuku City, Tokyo). All immunofluorescence wound sections were stained and imaged in the same batch, to better facilitate comparisons.

Statistics

Wound healing was measured using two different response variables: the amount of granulation tissue (measured in mm²) and the wound re-epithelialization, i.e., the diameter at the widest point of the wound after 7 days of healing subtracted from the initial wound opening (measured in mm). As granulation tissue is related to the thickness of the wound, while

wound extent is related to the wideness of the wound, these two response variables are not directly related to one another. All statistics were run using the open-source computing program R.

To assess whether the triple eGF therapy treatment has a statistically significant effect on wound healing or the composition of cells in a wound (Figs. 1 and 3–8), we used ANOVA tests, or (for cases when the ANOVA conditions were not met), we used Kruskal-Wallis tests. This involved testing the normality of the wound outcome data (wound extent and granulation tissue), using treatment as the explanatory variable, and testing that groups had approximately equal variances. Our ANOVA tests compare the mean cell percentages for each treatment, while Kruskal-Wallis tests compare the mean ranks between groups. Next, we ran post hoc tests to compare each treatment to the control, using a two-sample *t*-test (if samples were approximately normally distributed) or a Mann-Whitney test (if normality was not satisfied). In all cases, Bonferroni corrections for multiple comparisons were used.

We also compared the outcomes of WT GF treatments to their corresponding eGF treatment (e.g., VEGF vs VEGF-PIGF-2_{123–144}), denoted by # in Figs. 1 and 3–8. Each figure changes the response variable to a specific cell percentage. When the normality conditions were met, we carried out the comparison using two-sample *t*-tests (with independent populations). When the conditions were not met, we used Mann-Whitney tests.

To determine if the cellular milieu of a wound affects healing, we used exploratory data analysis, producing Table 1, followed by statistical tests to determine significance, with and without interaction terms. For each cell type (Figs. 3–8), we fit linear models using the percentage of live cells as our explanatory variable and wound outcomes (wound extent or granulation tissue) as the response, using scatterplots to confirm the linear relationship. We then fit linear models with wound area as the response variable.

We included covariates including mouse age, average glucose levels at the time of surgery, and whether or not the mouse had >400 mg/dl glucose in their lifetime. For both response variables, we fit multivariate linear regression models (confirming linear relationships using scatterplots) with and without interaction terms, to investigate the significance of these covariates. We determined that none of the covariates were statistically significant on their own or in combination, that the effect size of the triple

therapy treatment is far larger than that of the covariates, and that including interaction terms did not improve our models (except in cases of overfitting, identified and discarded using cross-validation), as measured by adjusted R^2 .

Reporting summary

Further information on research design is available in the Nature Research Reporting Summary linked to this article.

DATA AVAILABILITY

The datasets generated during the current study are available from the corresponding author on reasonable request.

Received: 9 March 2021; Accepted: 21 October 2021;

Published online: 18 November 2021

REFERENCES

- Ogurtsova, K. et al. IDF Diabetes Atlas: global estimates for the prevalence of diabetes for 2015 and 2040. *Diabetes Res. Clin. Pract.* **128**, 40–50 (2017).
- Singh, N., Armstrong, D. G. & Lipsky, B. A. Preventing foot ulcers in patients with diabetes. *JAMA* **293**, 217–228 (2005).
- Cook, J. J. & Simonson, D. C. *The Diabetic Foot* (Humana Press, 2012).
- Driver, V. R., Fabbri, M., Lavery, L. A. & Gibbons, G. The costs of diabetic foot: the economic case for the limb salvage team. *J. Am. Podiatr. Med. Assoc.* **100**, 335–341 (2010).
- Maahs, D. M., West, N. A., Lawrence, J. M. & Mayer-Davis, E. J. Epidemiology of type 1 diabetes. *Endocrinol. Metab. Clin. North Am.* **39**, 481–497 (2010).
- Center for Disease Control and Prevention. *National Diabetes Statistics Report: Estimates of Diabetes and its Burden in the United States* (US Department of Health and Human Services, 2014).
- American Diabetes Association. <http://www.diabetes.org/diabetes-basics/statistics/> (2021), accessed 02/02/2021.
- Black, E. et al. Decrease of collagen deposition in wound repair in type 1 diabetes independent of glycemic control. *Arch. Surg.* **138**, 34–40 (2003).
- Sen, C. K. et al. Human skin wounds: a major and snowballing threat to public health and the economy. *Wound Repair Regen.* **17**, 763–771 (2009).
- International Diabetes Federation. <https://www.idf.org/> (2015), accessed 05/05/2018.
- Blakytyn, R. & Jude, E. The molecular biology of chronic wounds and delayed healing in diabetes. *Diabet. Med.* **23**, 594–608 (2006).
- Xu, F., Zhang, C. & Graves, D. T. Abnormal cell responses and role of TNF- α in impaired diabetic wound healing. *BioMed. Res. Int.* **2013**, 754802 (2013).
- Briquez, P. S., Hubbell, J. A. & Martino, M. M. Extracellular matrix-inspired growth factor delivery systems for skin wound healing. *Adv. Wound Care* **4**, 479–489 (2015).
- Martino, M. M. & Hubbell, J. A. The 12th–14th type III repeats of fibronectin function as a highly promiscuous growth factor-binding domain. *FASEB J.* **24**, 4711–4721 (2010).
- Upton, Z. et al. Vitronectin: growth factor complexes hold potential as a wound therapy approach. *J. Invest. Dermatol.* **128**, 1535–1544 (2008).
- Julier, Z., Park, A. J., Briquez, P. S. & Martino, M. M. Promoting tissue regeneration by modulating the immune system. *Acta Biomater.* **53**, 13–28 (2017).
- Lauer, G. et al. Expression and proteolysis of vascular endothelial growth factor is increased in chronic wounds. *J. Invest. Dermatol.* **115**, 12–18 (2000).
- Babensee, J. E., McIntire, L. V. & Mikos, A. G. Growth factor delivery for tissue engineering. *Pharm. Res.* **17**, 497–504 (2000).
- Martino, M. M. et al. Growth factors engineered for super-affinity to the extracellular matrix enhance tissue healing. *Science* **343**, 885–888 (2014).
- Lee, K., Silva, E. A. & Mooney, D. J. Growth factor delivery-based tissue engineering: general approaches and a review of recent developments. *J. R. Soc. Interface* **8**, 153–170 (2011).
- Barrientos, S., Stojadinovic, O., Golinko, M. S., Brem, H. & Tomic-Canic, M. Growth factors and cytokines in wound healing. *Wound Repair Regen.* **16**, 585–601 (2008).
- Bennett, S. P., Griffiths, G. D., Schor, A. M., Leese, G. P. & Schor, S. L. Growth factors in the treatment of diabetic foot ulcers. *Br. J. Surg.* **90**, 133–146 (2003).
- Antoniades, H. N., Galanopoulos, T., Neville-Golden, J., Kiritsy, C. P. & Lynch, S. E. Injury induces in vivo expression of platelet-derived growth factor (PDGF) and PDGF receptor mRNAs in skin epithelial cells and PDGF mRNA in connective tissue fibroblasts. *Proc. Natl Acad. Sci. USA* **88**, 565–569 (1991).
- Bao, P. et al. The role of vascular endothelial growth factor in wound healing. *J. Surg. Res.* **153**, 347–358 (2009).
- Brown, L. F. et al. Expression of vascular permeability factor (vascular endothelial growth factor) by epidermal keratinocytes during wound healing. *J. Exp. Med.* **176**, 1375–1379 (1992).
- Galiano, R. D. et al. Topical vascular endothelial growth factor accelerates diabetic wound healing through increased angiogenesis and by mobilizing and recruiting bone marrow-derived cells. *Am. J. Pathol.* **164**, 1935–1947 (2004).
- Dao, D. T., Anez-Bustillos, L., Adam, R. M., Puder, M. & Bielenberg, D. R. Heparin-binding epidermal growth factor-like growth factor as a critical mediator of tissue repair and regeneration. *Am. J. Pathol.* **188**, 2446–2456 (2018).
- Edwards, J. P., Zhang, X. & Mosser, D. M. The expression of heparin-binding epidermal growth factor-like growth factor by regulatory macrophages. *J. Immunol.* **182**, 1929–1939 (2009).
- Shirakata, Y. et al. Heparin-binding EGF-like growth factor accelerates keratinocyte migration and skin wound healing. *J. Cell Sci.* **118**, 2363–2370 (2005).
- Puccinelli, T. J., Bertics, P. J. & Masters, K. S. Regulation of keratinocyte signaling and function via changes in epidermal growth factor presentation. *Acta Biomater.* **6**, 3415–3425 (2010).
- Yamasaki, K. et al. Keratinocyte growth inhibition by high-dose epidermal growth factor is mediated by transforming growth factor beta autoinduction: a negative feedback mechanism for keratinocyte growth. *J. Invest. Dermatol.* **120**, 1030–1037 (2003).
- Traversa, B. & Sussman, G. The role of growth factors, cytokines and proteases in wound management. *Prim. Intent.* **9**, 161–167 (2001).
- Buchberger, B. et al. The effectiveness of interventions in workplace health promotion as to maintain the working capacity of health care personal. *GMS Health Technol. Assess.* **7**, Doc06 (2011).
- Chan, R. K. et al. Effect of recombinant platelet-derived growth factor (Regranex) on wound closure in genetically diabetic mice. *J. Burn Care Res.* **27**, 202–205 (2006).
- Fang, R. C. & Galiano, R. D. A review of becaplermin gel in the treatment of diabetic neuropathic foot ulcers. *Biologics* **2**, 1–12 (2008).
- Papanas, N. & Maltezos, E. Benefit-risk assessment of becaplermin in the treatment of diabetic foot ulcers. *Drug Saf.* **33**, 455–461 (2010).
- Brem, H. & Tomic-Canic, M. Cellular and molecular basis of wound healing in diabetes. *J. Clin. Invest.* **117**, 1219–1222 (2007).
- Tsourdji, E., Barthel, A., Rietzsch, H., Reichel, A. & Bornstein, S. R. Current aspects in the pathophysiology and treatment of chronic wounds in diabetes mellitus. *Biomed. Res. Int.* **2013**, 385641 (2013).
- Gurtner, G. C., Werner, S., Barrandon, Y. & Longaker, M. T. Wound repair and regeneration. *Nature* **453**, 314–321 (2008).
- Leibovich, S. J. & Ross, R. The role of the macrophage in wound repair. A study with hydrocortisone and antimacrophage serum. *Am. J. Pathol.* **78**, 71–100 (1975).
- Wynn, T. A. & Vannella, K. M. Macrophages in tissue repair, regeneration, and fibrosis. *Immunity* **44**, 450–462 (2016).
- Campbell, L., Saville, C. R., Murray, P. J., Cruickshank, S. M. & Hardman, M. J. Local arginase 1 activity is required for cutaneous wound healing. *J. Invest. Dermatol.* **133**, 2461–2470 (2013).
- Brancato, S. K. & Albina, J. E. Wound macrophages as key regulators of repair: origin, phenotype, and function. *Am. J. Pathol.* **178**, 19–25 (2011).
- Arpaia, N. et al. A distinct function of regulatory T cells in tissue protection. *Cell* **162**, 1078–1089 (2015).
- Nosbaum, A. et al. Cutting edge: regulatory T cells facilitate cutaneous wound healing. *J. Immunol.* **196**, 2010–2014 (2016).
- Bodnar, R. J., Satish, L., Yates, C. C. & Wells, A. Pericytes: a newly recognized player in wound healing. *Wound Repair Regen.* **24**, 204–214 (2016).
- Babad, J., Geliebter, A. & DiLorenzo, T. P. T-cell autoantigens in the non-obese diabetic mouse model of autoimmune diabetes. *Immunology* **131**, 459–465 (2010).
- Alonso, L. & Fuchs, E. The hair cycle. *J. Cell Sci.* **119**, 391–393 (2006).
- Moya, A. et al. Human mesenchymal stem cell failure to adapt to glucose shortage and rapidly use intracellular energy reserves through glycolysis explains poor cell survival after implantation. *Stem Cells* **36**, 363–376 (2018).
- Nikolic, T., Bunk, M., Drexhage, H. A. & Leenen, P. J. Bone marrow precursors of nonobese diabetic mice develop into defective macrophage-like dendritic cells in vitro. *J. Immunol.* **173**, 4342–4351 (2004).
- Serreze, D. V., Gaskins, H. R. & Leiter, E. H. Defects in the differentiation and function of antigen presenting cells in NOD/Lt mice. *J. Immunol.* **150**, 2534–2543 (1993).
- Dunn, L. et al. Murine model of wound healing. *J. Vis. Exp.* **75**, e50265, <https://doi.org/10.3791/50265> (2013).

ACKNOWLEDGEMENTS

We thank the Human Tissue Resource Center of the University of Chicago for histology analysis. We thank the Integrated Light Microscopy Core of the University of Chicago for Imaging.

This work was supported in part by the National Institutes of Health, National Institute of Diabetes and Digestive and Kidney Diseases grant DP3DK108215 (to J.A.H.), by the Searle Funds at The Chicago Community Trust through the Chicago Biomedical Consortium (C-080, to J.A.H.), and by the University of Chicago (to J.A.H.).

AUTHOR CONTRIBUTIONS

M.W., P.S.B., and J.A.H. designed the project. M.W. performed experiments. M.W., P.S.B., and D.W. analyzed data. M.W. and J.A.H. wrote the paper. All authors read and approved the final manuscript.

COMPETING INTERESTS

P.S.B. and J.A.H. are inventors on U.S. Patent US9,879,062. The other authors declare no competing interests.

ADDITIONAL INFORMATION

Supplementary information The online version contains supplementary material available at <https://doi.org/10.1038/s41536-021-00189-1>.

Correspondence and requests for materials should be addressed to Jeffrey A. Hubbell.

Reprints and permission information is available at <http://www.nature.com/reprints>

Publisher's note Springer Nature remains neutral with regard to jurisdictional claims in published maps and institutional affiliations.



Open Access This article is licensed under a Creative Commons Attribution 4.0 International License, which permits use, sharing, adaptation, distribution and reproduction in any medium or format, as long as you give appropriate credit to the original author(s) and the source, provide a link to the Creative Commons license, and indicate if changes were made. The images or other third party material in this article are included in the article's Creative Commons license, unless indicated otherwise in a credit line to the material. If material is not included in the article's Creative Commons license and your intended use is not permitted by statutory regulation or exceeds the permitted use, you will need to obtain permission directly from the copyright holder. To view a copy of this license, visit <http://creativecommons.org/licenses/by/4.0/>.

© The Author(s) 2021